Luminescent hydrogel based on a new Au(I) complex

Raquel Gavara,[a] Jordi Llorca,[b] João Carlos Lima,[a] and Laura Rodríguez [c,*]

[a] *REQUIMTE, Departamento de Química, CQFB, Universidade Nova de Lisboa, Monte de Caparica, Portugal.*

[b] *Institut de Tècniques Energètiques i Centre de Recerca en NanoEnginyeria, Universitat Politècnica de Catalunya, Diagonal 647,08028 Barcelona, Spain*

[c] *Departament de Química Inorgànica, Universitat de Barcelona, Barcelona, Spain.*

Fax: +34 934907725; Tel.: +34 934031136;

e-mail address: laura.rodriguez@qi.ub.es

Supplementary Information

Experimental Section

General Procedures. All manipulations were performed under prepurified N_2 using standard Schlenk techniques. All solvents were distilled from appropriate drying agents. Commercial reagent 1,3,5-triaza-7-phosphaadamantane (PTA, Aldrich 97%) was used as received. Literature methods were used to prepare [AuCl(tht)],[1] $[Au(C{\equiv}C\text{-}C_5H_4N)]_n$,[2] $NC_5H_4C{\equiv}CH$.[3]

Physical Measurements. Infrared spectra were recorded on a FT-IR 520 Nicolet Spectrophotometer. ^1H NMR (δ(TMS) = 0.0 ppm), $^{31}P\{^1H\}$-NMR (δ (85% H_3PO_4) = 0.0 ppm) spectra were obtained on a Varian Unity 400 and Varian Inova 300. Elemental analyses of C, H, N and S were carried out at the Serveis Científico-Tècnics in Barcelona. ES(+) mass spectra were recorded on a Fisons VG Quatro spectrometer. Absorption spectra were recorded on a Varian Cary 100 Bio UV-spectrophotometer and emission spectra on a Horiba-Jobin-Yvon SPEX Fluorolog 3.22 and Nanolog spectrofluorimeters. The emission quantum yields were recorded with an integrating sphere accessory for a Horiba-Jobin–Yvon SPEX Fluorolog 3.22 spectrofluorimeter. Fluorescence decays. The samples were excited at 280 nm using a nanoled (IBH).The electronic start pulses were shaped in a constant fraction discriminator (Canberra 2126) and directed to a time to amplitude converter (TAC, Canberra 2145). Emission wavelength (450 nm) was selected by a monochromator (Oriel 77250) imaged in a fast photomultiplier (9814B Electron Tubes Inc.), the PM signal was shaped as before and delayed before entering the TAC as stop pulses. The analogue TAC signals were digitized (ADC, ND582) and stored in multichannel analizer installed in a PC (1024 channels, 1.95 ns/ch). The analysis of the decays was carried out with the method of modulating functions extended by global analysis as implemented by Striker *et al.*[4] Microspectrofluorimetry measurements were obtained with a microSPEX instrument where the Spex Fluorog apparatus 3.22 is connected to an Olympus BX51 M confocal microscope, with spatial resolution controlled with a multiple-pinhole turret, corresponding to a minimum 2 μm and maximum 60 μm spot with a 50× lens.[5] Fluorescence microscopy was recorded on an Axioplan 2ie Zeiss imaging microscope equipped with a NikonDXM1200F digital camera. Excitation light for fluorescence imaging was selected using filters in the range 395-440 nm and 510-560 nm respectively.

Scanning electron microscopy (SEM) was carried out at 5 kV using a Neon40 Crossbeam Station (Zeiss) equipped with a field emission gun and an energy-dispersive X-ray detector (EDX). Optical interferometry images were obtained with a Veeco Wyko 9300NT instrument.

Power x-ray diffraction was carried out on a PANalytical X'Pert PRO MPD θ/θ powder diffractometer of a 240 millimetre radius, in a configuration of convergent beam with a focalizing mirror and a transmission geometry with flat samples sandwiched between low absorbing films.

Synthesis of [(PTA)Au(C≡C-C_5H_4N)]

Solid PTA (22mg, 0.13 mmol) was added to a suspension of $[Au(C\equiv C\text{-}C_5H_4N)]_n$ (40 mg, 0.13 mmol) in CH_2Cl_2 (15 ml). After 30 min of stirring at room temperature, the resulting pale yellow solution was concentrated (5ml), and diethyl ether (10ml) was added to precipitate a pale yellow solid. Yield: 56 mg, 95%. ^{1}H NMR (250.1 MHz, $CDCl_3$): 8.46 (d, *J* = 5.2 Hz, 2H, $H_{\alpha\text{-pyr}}$), 7.26 (d, *J* = 5.2 Hz, 2H, $H_{\beta\text{-pyr}}$), 4.52-4.40 (AB q, J = 12.0 Hz, 6H, N-CH_2-N), 4.17 (s, 6H, N-CH_2-P). ^{31}P{^{1}H}NMR (101.3 MHz, $CDCl_3$): -51.8 (s, PTA). IR (KBr, cm^{-1}): 2919 (CH_2), 2115 (C≡C), 1588 (C=N). ES-MS(+) *m/z*: 457.1 ($[M+H^+]^+$, calc.: 457.1). Anal. Calcd. for $C_{13}H_{16}AuN_4P$: C, 34.22; H, 3.53; N, 12.28. Found: C, 34.24; H, 3.56; N, 12.30.

Preparation of the gel

Solid [(PTA)Au(C≡C-C_5H_4N)] was dissolved in water in different concentrations range (0.015-0.05% weight). The sample was maintained under sonication for *ca*. 20 minutes and left at room temperature at least for 4 hours.

[1] R. Usón, A. Laguna, *Organometallic Synthesis*; King, R. B., Eisch, J. J., Eds.; Elsevier: Amsterdam, 1986; Vol. 3, p 322.

[2] M. Ferrer, M. Mounir, L. Rodríguez, O. Rossell, S. Coco, P. Gómez-Sal, A. Martin, *J. Organomet. Chem.* 2005, **690**, 2200.

[3] L. Dellaciana, A. Haim, *J. Heterocycl. Chem.* 1984, **21**, 607.

[4] G. Striker, V. Subramaniam, C.A.M. Seidel, A. Volkmer, *J. Phys. Chem. B*, 1999, **103**, 8612.

[5] M.J. Melo, A. Claro, *Acc. Chem. Res.*, 2010, **43**, 857.

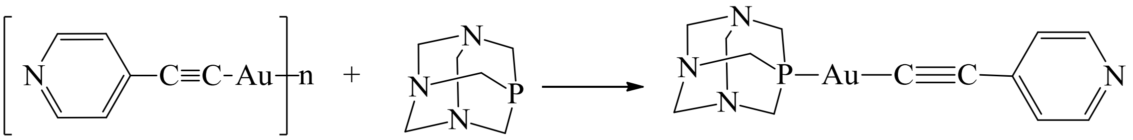

Scheme S1. Synthesis of [(PTA)Au(C≡C-C_5H_4N)]

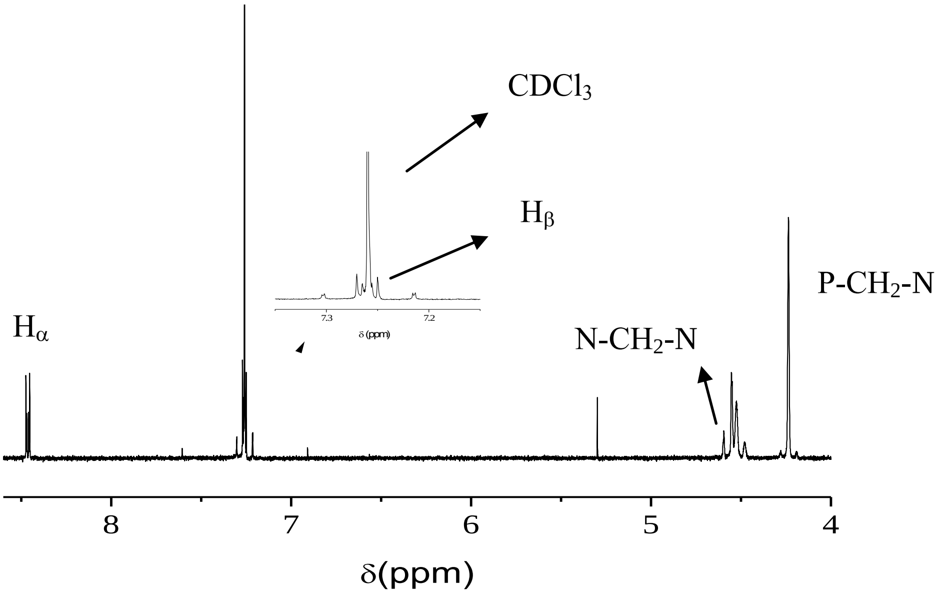

Figure S1. ^{1}H-NMR spectrum of [(PTA)Au(C≡C-C_5H_4N)] in $CDCl_3$.

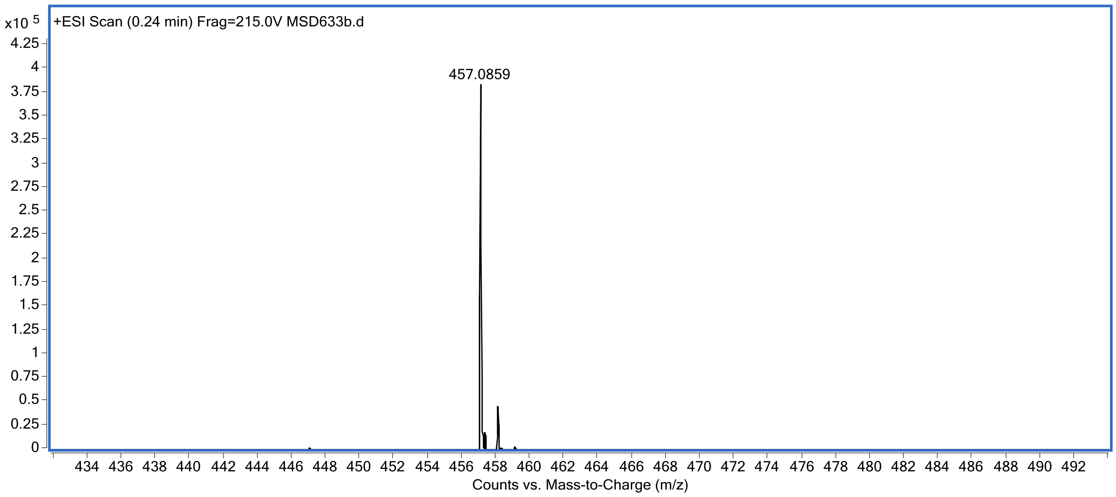

Figure S2. ESI-MS(+) spectrum of [(PTA)Au(C≡C-C_5H_4N)].

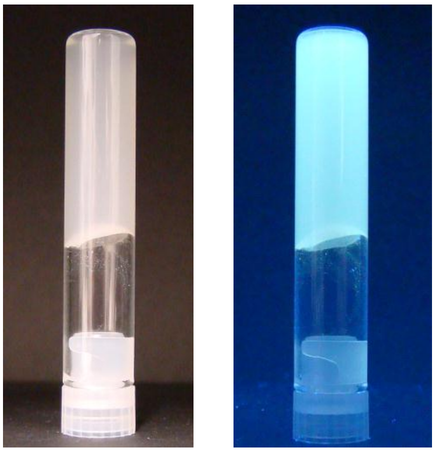

Figure S3. Gel texture of [(PTA)Au(C≡C-C_5H_4N)] in water under visible (left) and UV light (right).

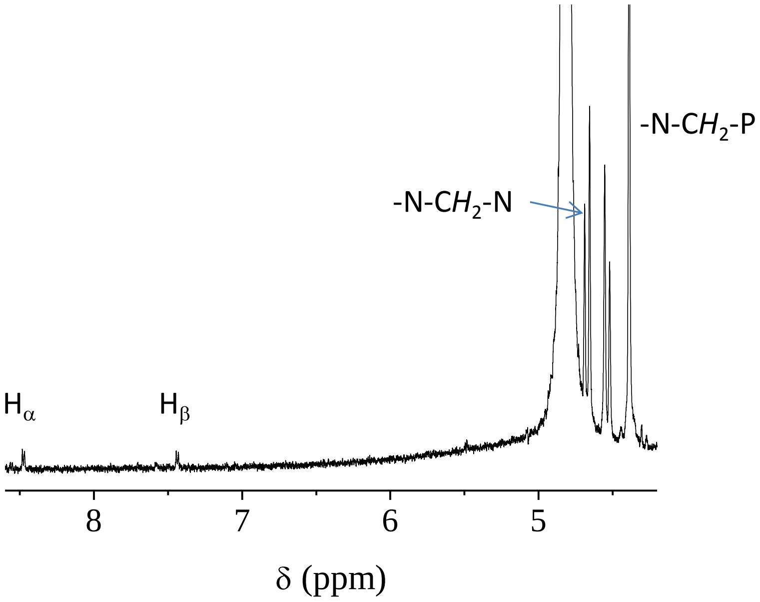

Figure S4. ^{1}H-NMR of [(PTA)Au(C≡C-C_5H_4N)] under gel conditions in D_2O.

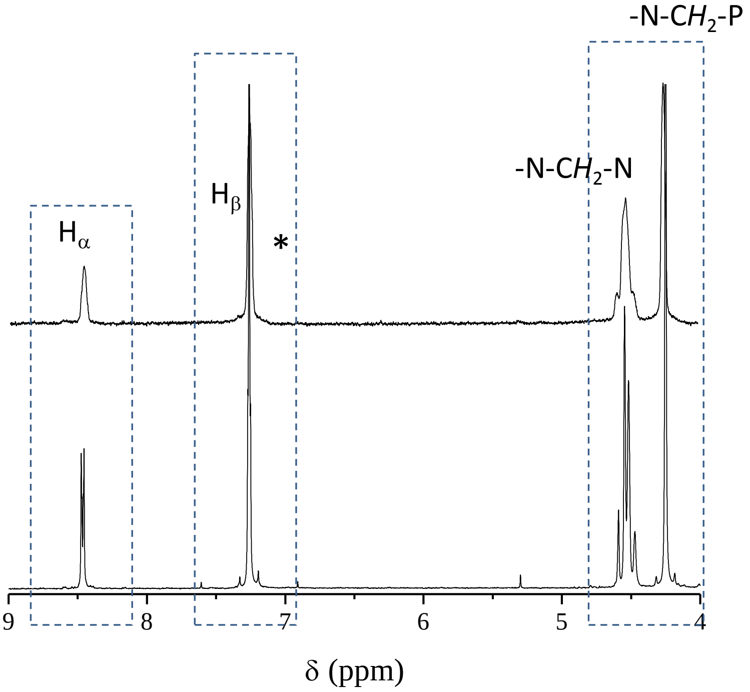

Figure S5. ^{1}H-NMR spectra of [(PTA)Au(C≡C-C_5H_4N)] in $CDCl_3$ at different concentrations. * H_β protons are buried under $CDCl_3$.

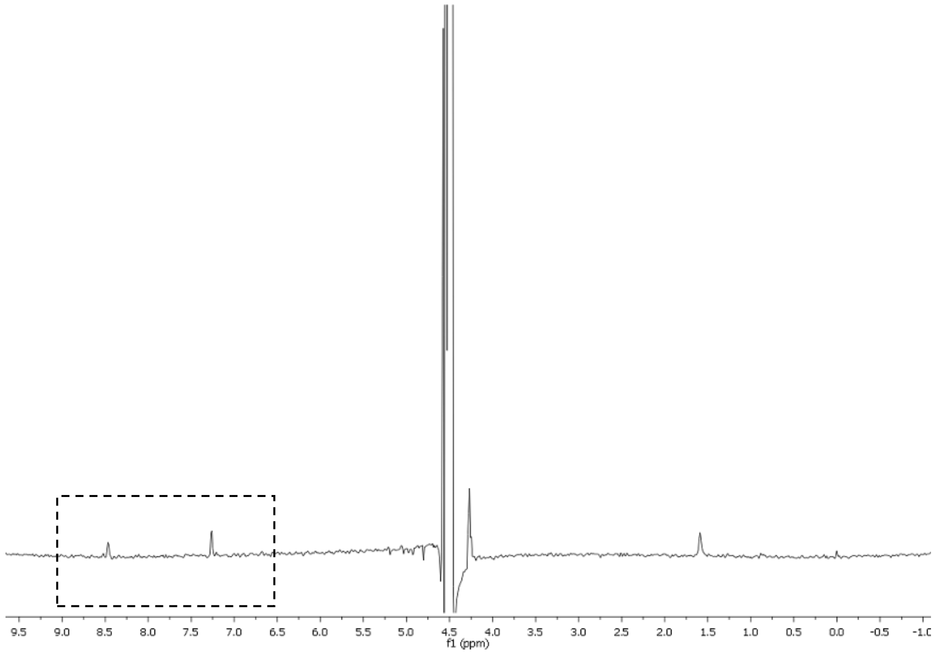

Figure S6. Trace NMR image retrieved from NOESY interactions of N-CH_2-N protons.

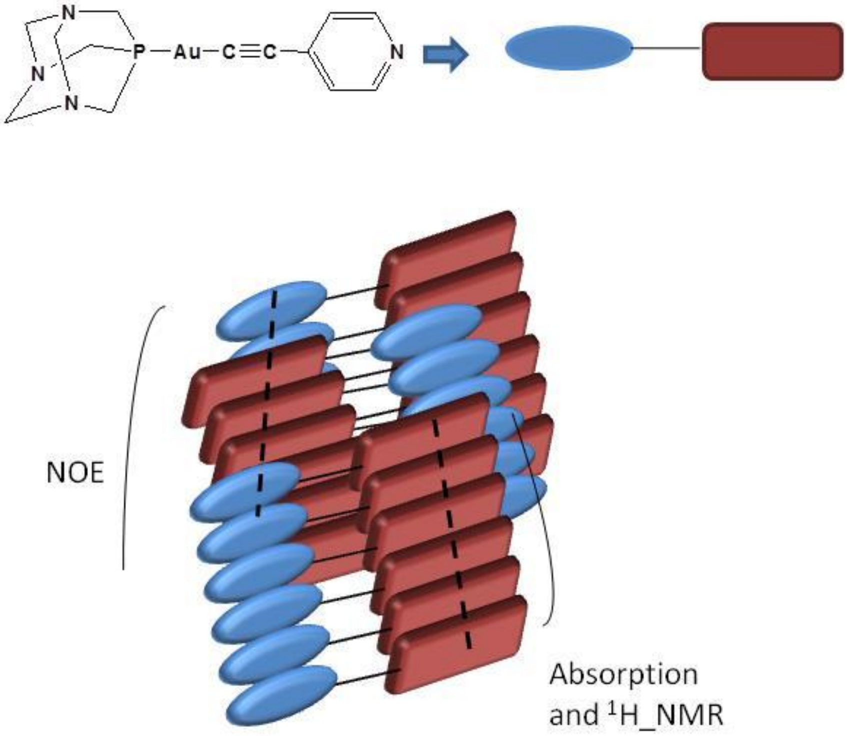

Figure S7. Schematic representation of the possible 3D disposition of [(PTA)Au(C≡C-C_5H_4N)].

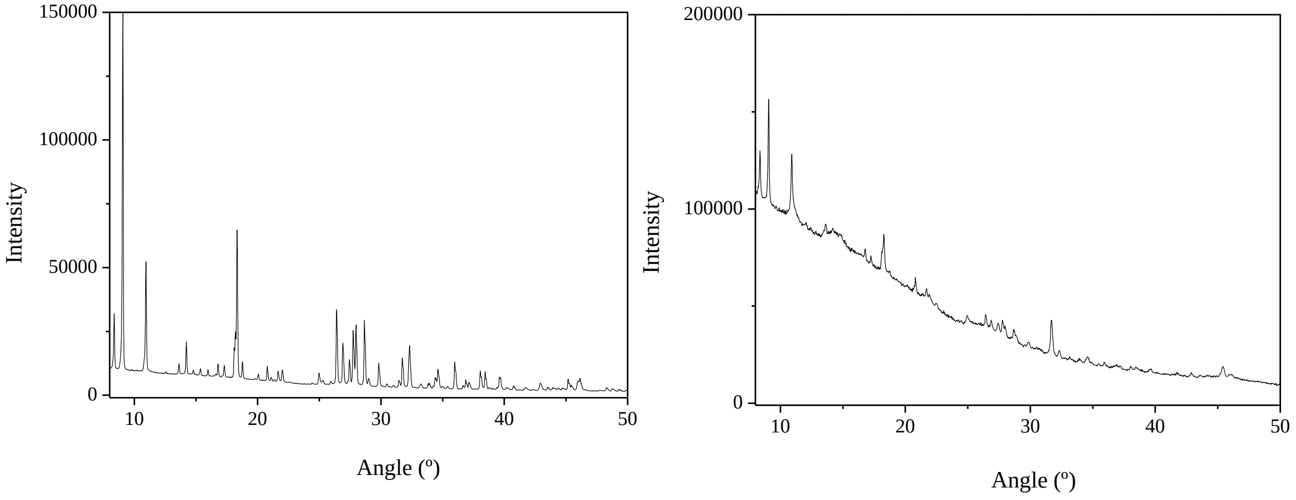

Figure S8. DRX of [(PTA)Au(C≡C-C_5H_4N] solid (left) and xerogel (x5, right).

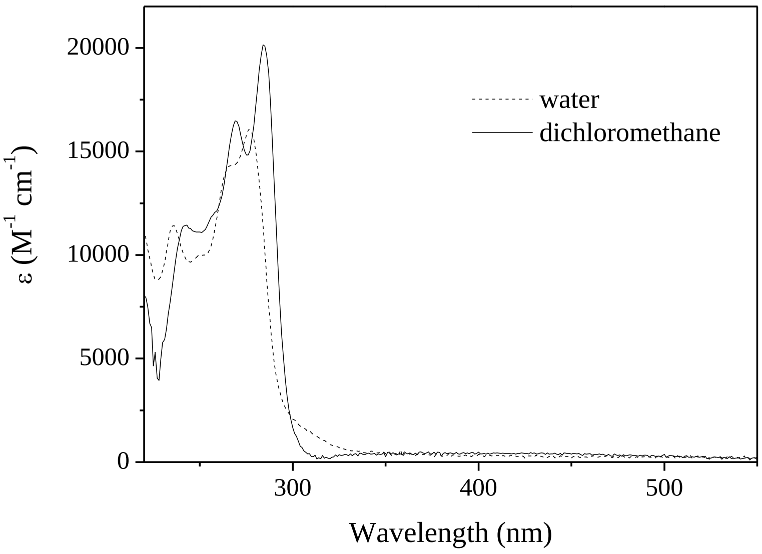

Figure S9. Normalized absorption spectra of a 1x10^{-5}M solution of [(PTA)Au(C≡C-C_5H_4N)] in dichloromethane (solid line) and water (dashed line).

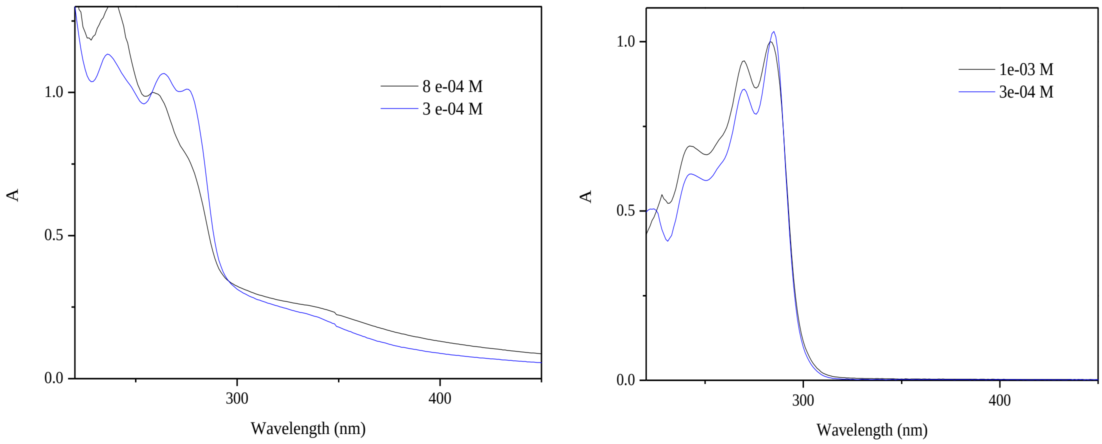

Figure S10. Normalized absorption spectra of [(PTA)Au(C≡C-C_5H_4N)] in water (left) dichloromethane (right) at different concentrations (the samples were incubated for three days).

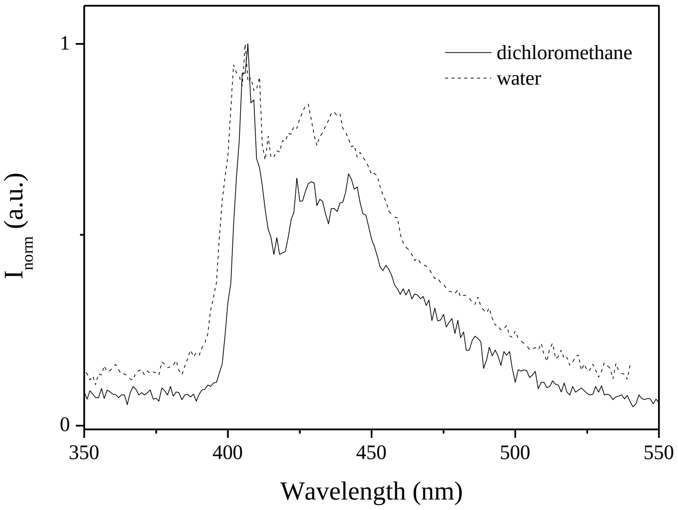

Figure S11. Normalized solution emission spectra of [(PTA)Au(C≡C-C_5H_4N)] in water and dichloromethane at 298 K (λ_{exc} = 280 nm).

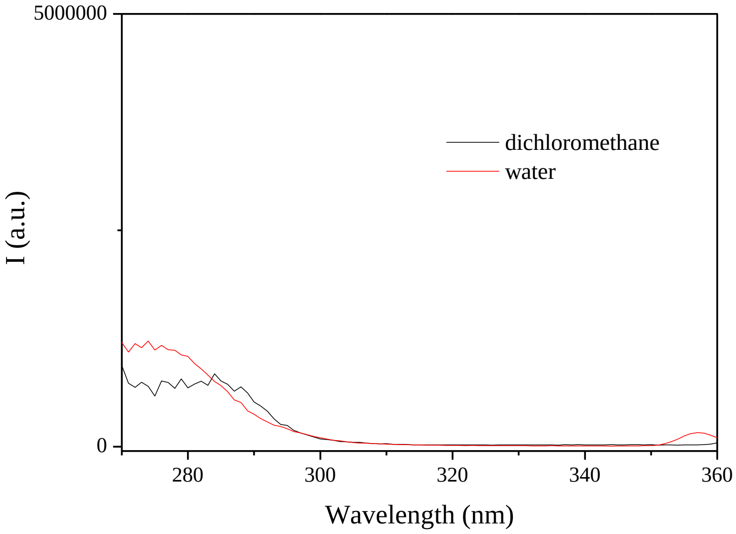

Figure S12. Excitation spectrum of [(PTA)Au(C≡C-C_5H_4N)] in dichoromethane and in water ($1x10^{-5}$M concentration). λ_{em} = 420 nm.

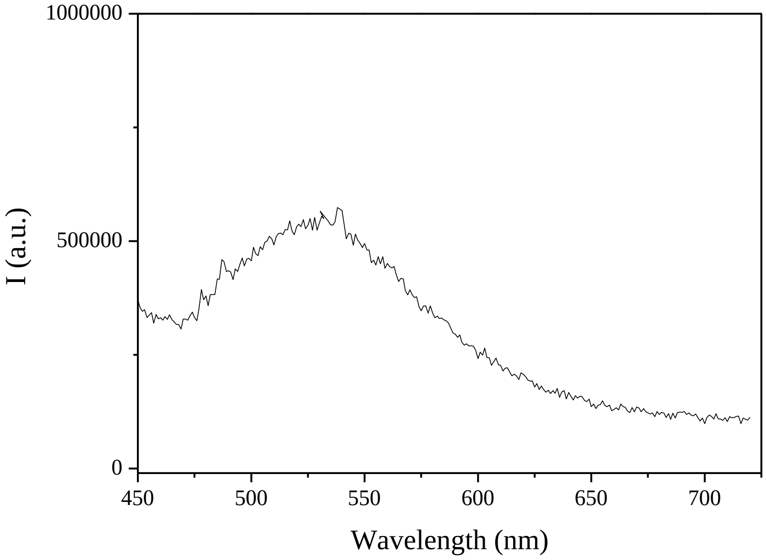

Figure S13. Solid emission spectrum of [(PTA)Au(C≡C-C_5H_4N)]. λ_{exc} = 360 nm.

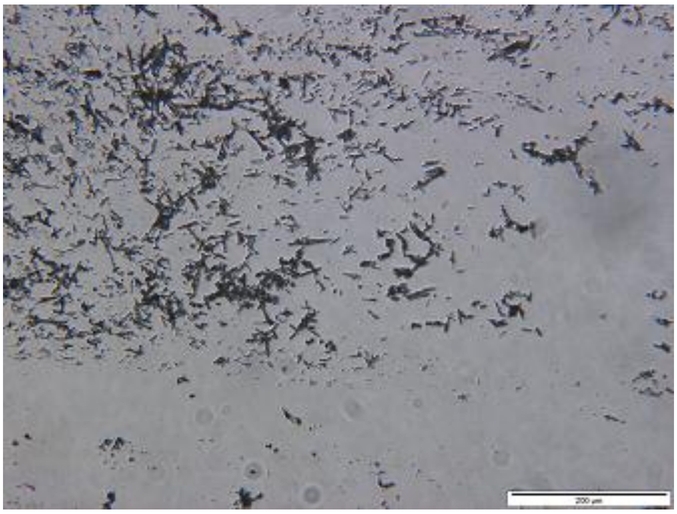

Figure S14. Images of amorphous solid [(PTA)Au(C≡C-C_5H_4N)] under optical microscopy.

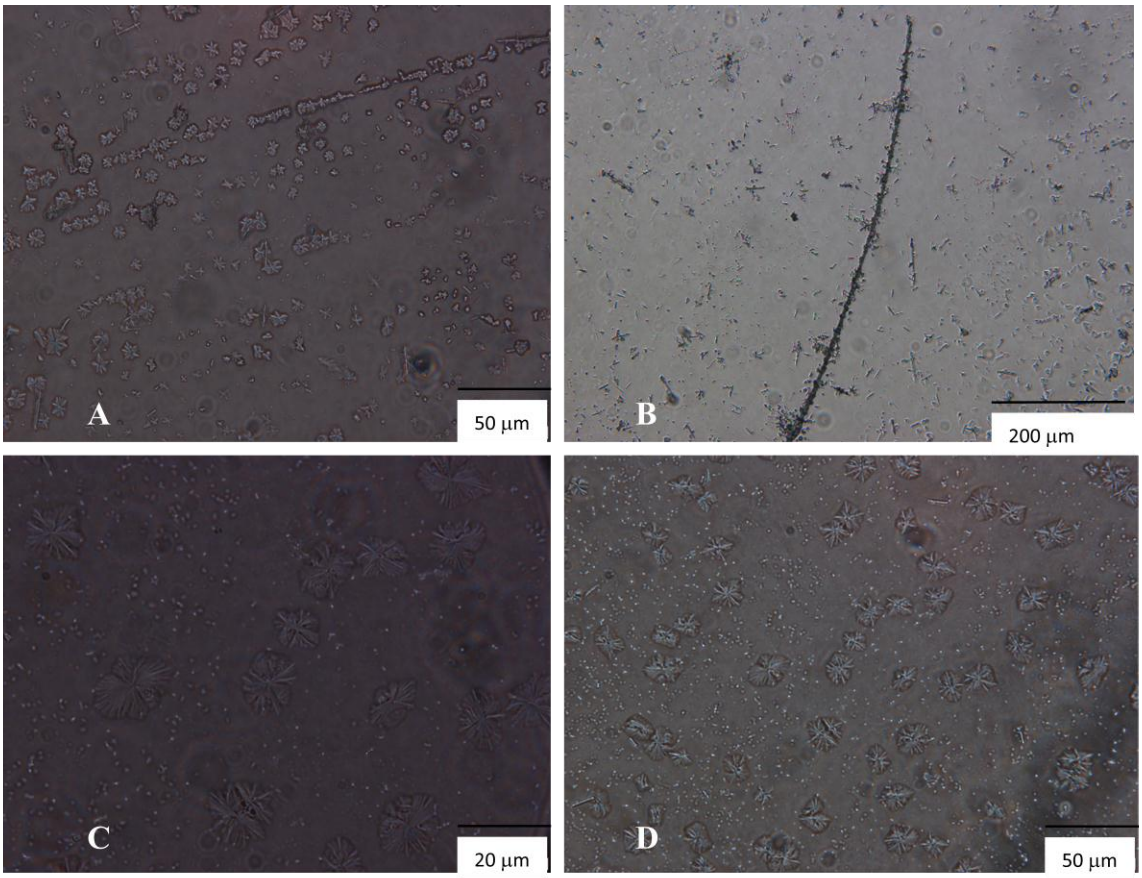

Figure S15. Images of [(PTA)Au(C≡C-C_5H_4N)] xerogel under optical microscopy.

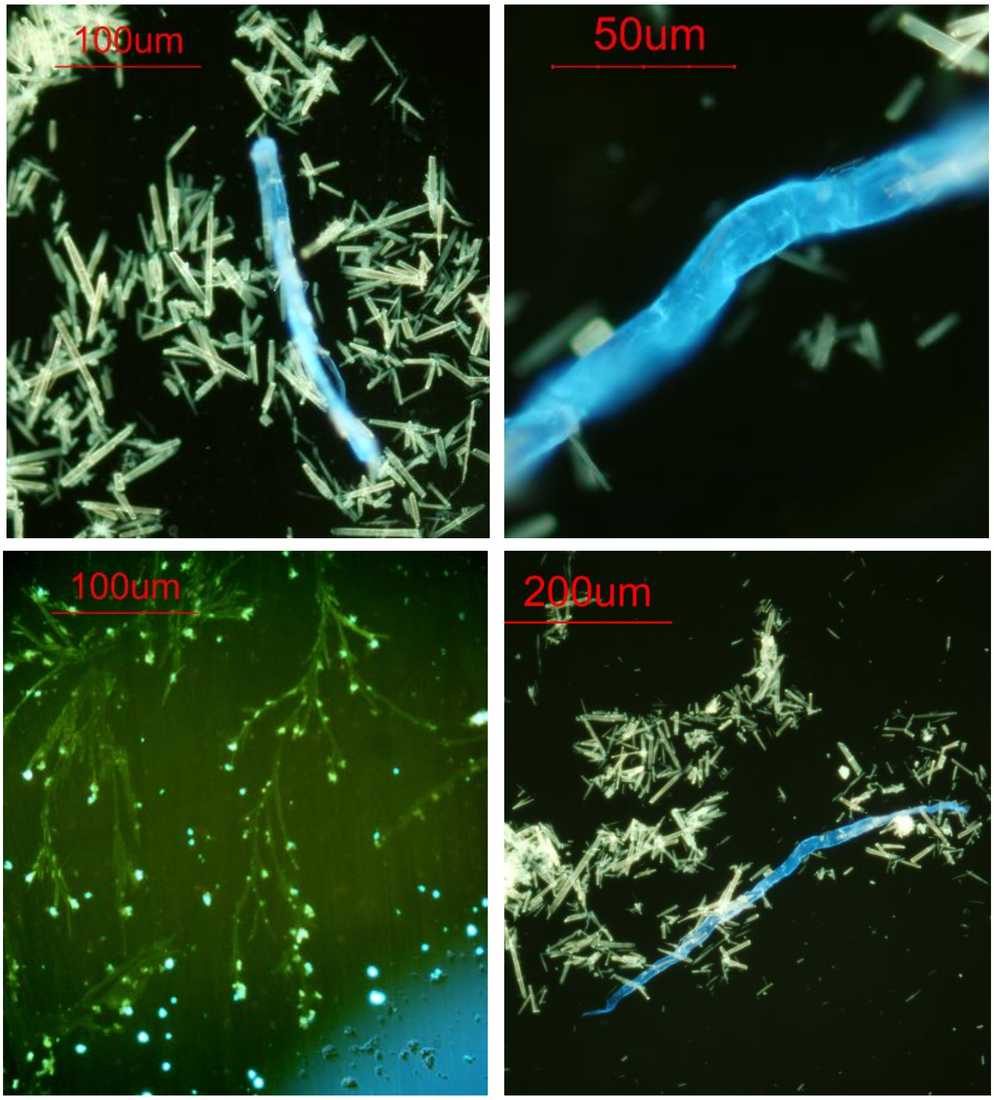

Figure S16. Images of [(PTA)Au(C≡C-C_5H_4N)] xerogel under fluorescence optical microscopy with a 395-440 nm filter.

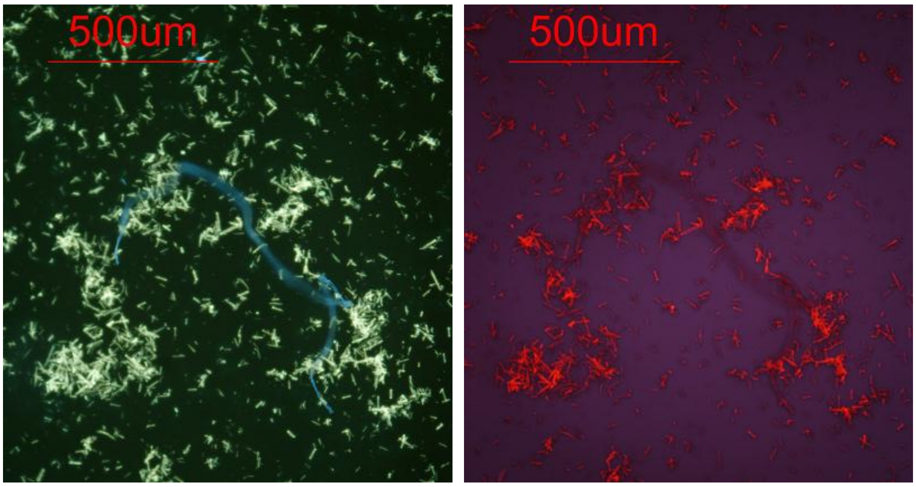

Figure S17. Images of [(PTA)Au(C≡C-C_5H_4N)] xerogel under fluorescence optical microscopy with a 395-440 nm filter (left) and 510-560 nm filter (right).

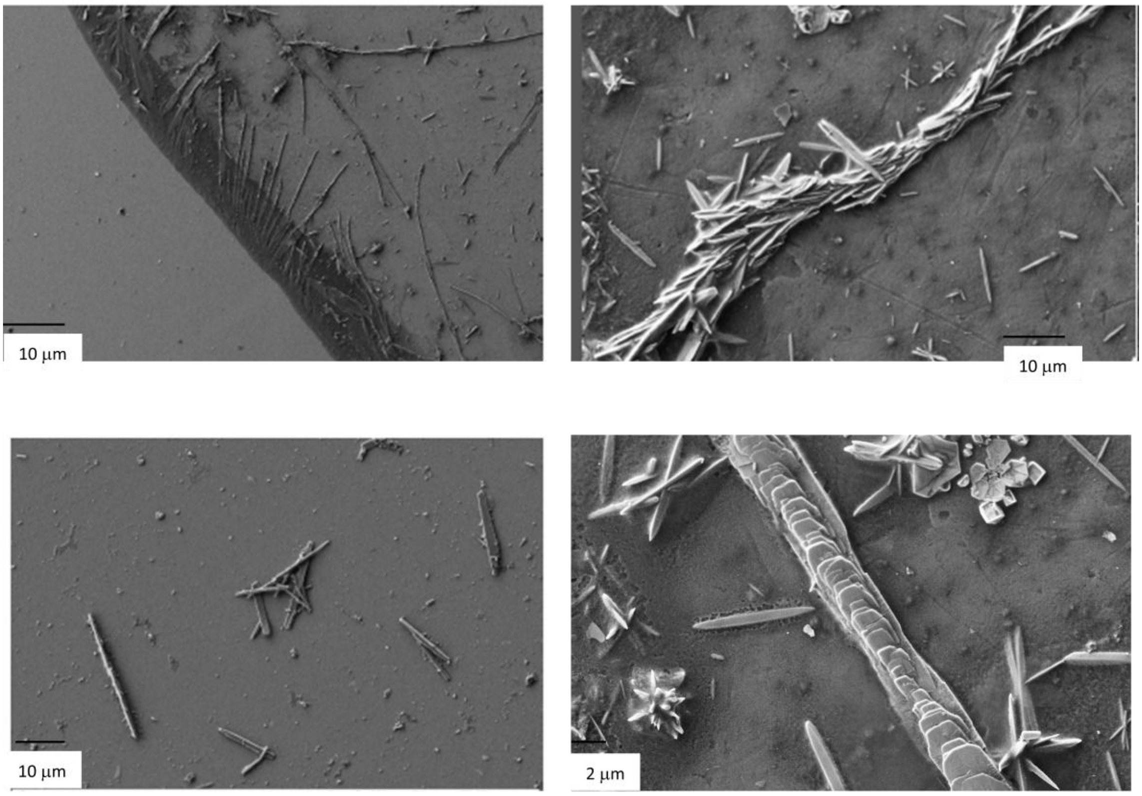

Figure S18. SEM images of [(PTA)Au(C≡C-C_5H_4N)] xerogel recorded with secondary electrons showing the fibers at different magnifications. Sample was prepared by cast-dropping on a Si substrate.

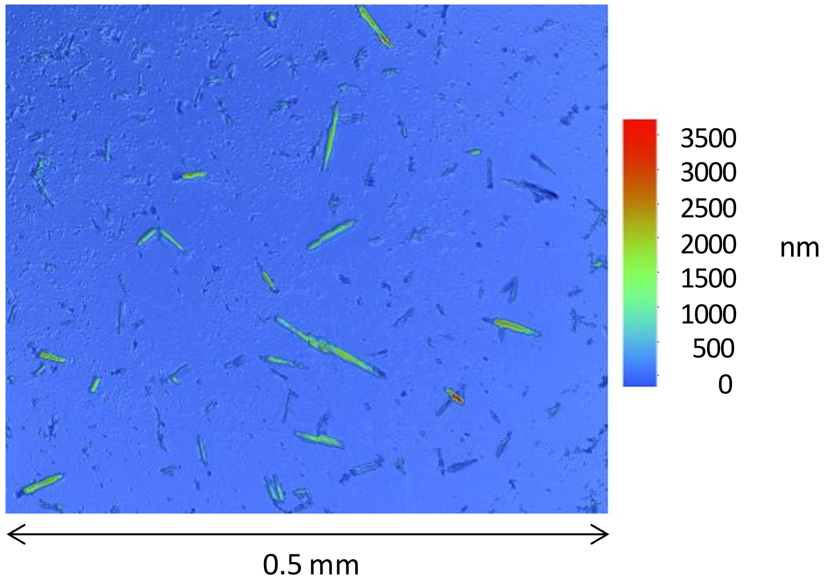

Figure S19. Optical interferometric image of [(PTA)Au(C≡C-C_5H_4N)] xerogel.

Stability studies of the gel (Annex 1)

Absorption spectra of a $1x10^{-3}$M concentration of the gelified sample (incubated for 4 hours) were recorded at different temperatures (20 – 80 ºC). The results are shown in Figure S20.

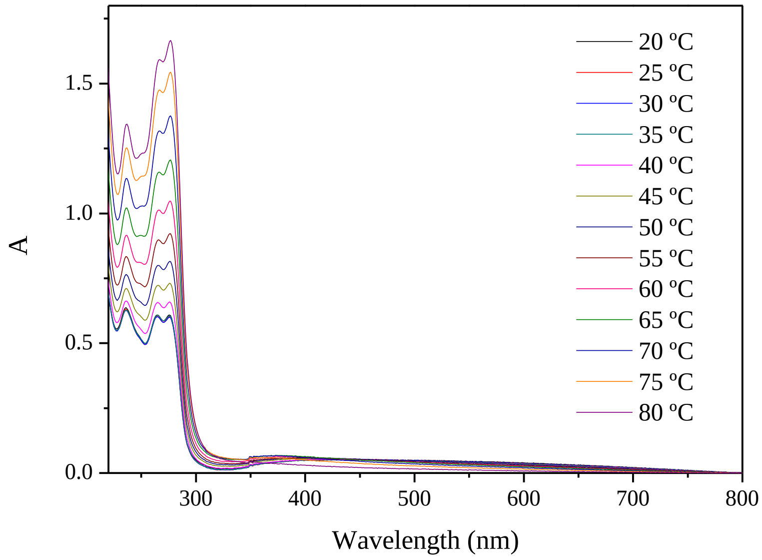

Figure S20. Electronic absorption spectra of a $1x10^{-3}$M sample of [(PTA)Au(C≡C-C_5H_4N)] in water at different temperatures.

The ratio between the absorbances at 275nm and 264 nm decreases when aggregation occurs (see Fig. S10 left). This ratio increases by heating the sample, indicative of desaggregation.

The plot of A275nm/A264nm against temperature shows a sigmoid trend that let us to calculate the T_{50}, i.e. melting temperature as 54 ºC (Figure S21).

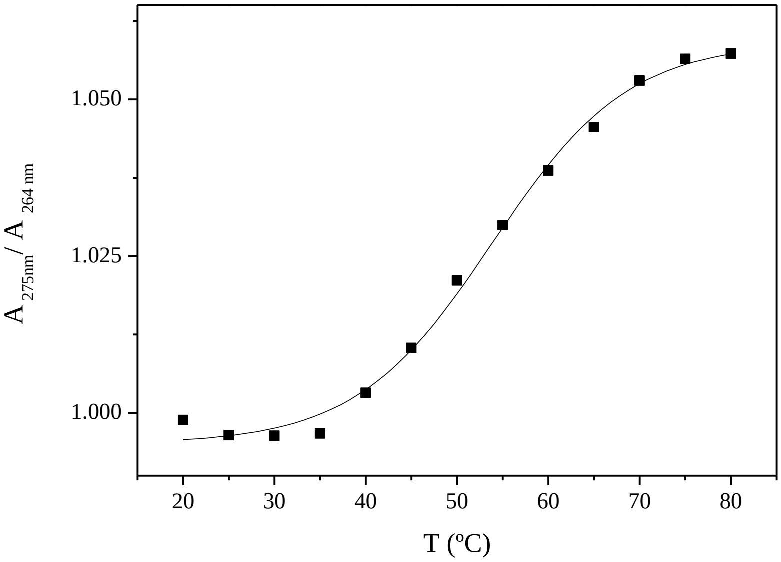

Figure S21. Plot of the A_{275nm}/A_{264nm} ratio against temperature for a $1x10^{-3}$M concentration sample.

The same experiments were recorded with a $5x10^{-4}$M concentration and the results summarized in figures S22 and S23.

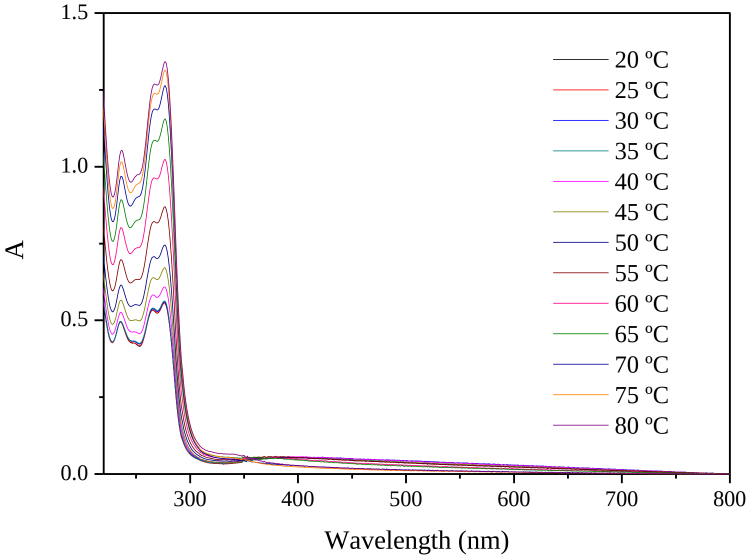

Figure S22. Electronic absorption spectra of a $5x10^{-4}$M sample of [(PTA)Au(C≡C-C_5H_4N)] in water at different temperatures.

The ratio between A275nm/A264 nm was plotted against temperature and the results follow a sigmoid trend that let us to calculate the T_{50}, i.e. melting temperature as 50 ºC (Figure S23). It is observed that the lowest the concentration the lowest the melting temperature of the sample.

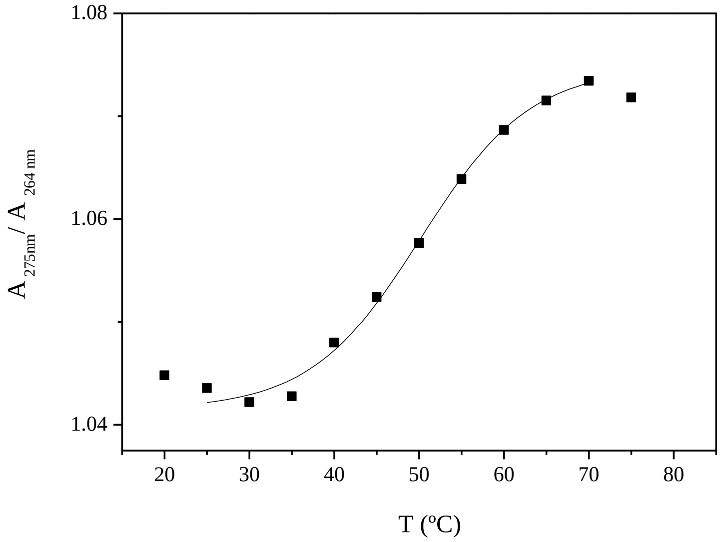

Figure S23. Plot of the A_{275nm}/A_{264nm} ratio against temperature for a $5x10^{-4}M$ concentration sample

Looking at Figure S21 and S23, it seems that the aggregation process that induces gelation completely disappears at 80ºC ($1x10^{-3}M$) and 70 ºC ($5x10^{-4}M$). This fact has been also verified by ^1H-NMR experiments recorded at 25 ºC, 45 ºC, 65 ºC and 80 ºC in D_2O at $1x10^{-3}M$ concentration. The results are shown in Figure S24. It could be seen that at room temperature, the formation of different aggregates seems to exist according to the different environments of the pyridyl protons. These different environments completely disappear at 80 ºC where we can observe a symmetric environment for these protons.

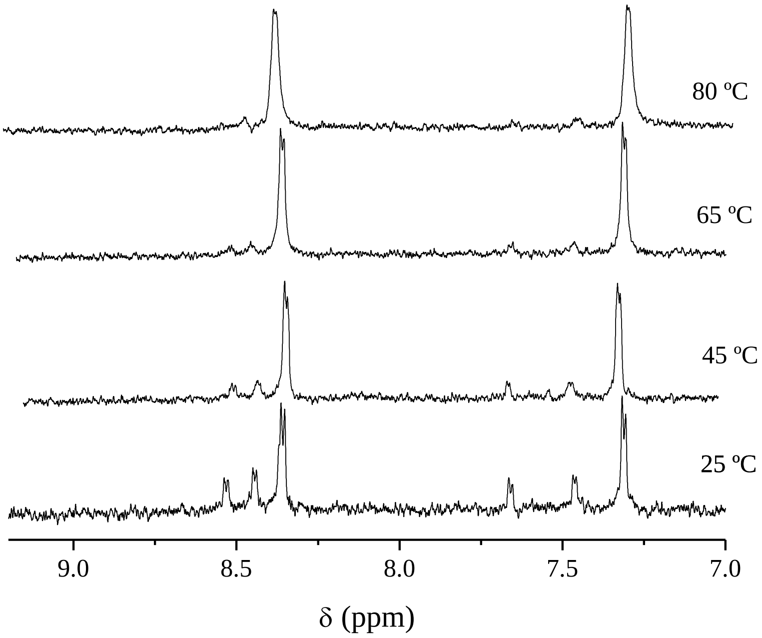

Figure S24. ^{1}H-NMR spectra of a 1x10^{-3}M sample in D_2O.

[PTA-AuC≡C-C_5H_4N]						
H_2O			CH_2Cl_2			Solid
Absorption λ_{max}, nm (10^{-3} ε, $M^{-1} \cdot cm^{-1}$)	**Emission, RT (λ_{max}, nm)**	**Emission 77K (λ_{max}, nm)**	**Absorption λ_{max}, nm (10^{-3} ε, $M^{-1} \cdot cm^{-1}$)**	**Emission RT (λ_{max}, nm)**	**Emission 77K (λ_{max}, nm)**	**Emission (λ_{max}, nm)**
235 (11.1) 265 (14.0), 277 (15.8), 330 (6.4)	406, 423, 441, 480 sh	433, 555	242 (11.4), 269 (16.5), 284 (20.1)	407, 428, 445 480 sh	407, 430, 450, 510	535

Table S1. Absorption and emission (λ_{exc}= 280) data of [(PTA)Au(C≡C-C_5H_4N)] (1x10^{-5} M).